The Growth Process, Stability of GaP Nanocrystals and Formation of Ga_3P Nanocrystals under Solvothermal Conditions in Benzene

Shanmin Gao,[a] Jun Lu,[a] Yan Zhao,[a] Nan Chen,[a] and Yi Xie*[a]

Keywords: Gallium / Phosphides / Nanostructures / Solvothermal synthesis

The growth process, stability of GaP nanocrystals and the formation of Ga_3P nanocrystals under solvothermal conditions were investigated. At moderate reaction times and temperature, the growth process is mainly in accordance with the Ostwald ripening mechanism, which is the dissolving of the smaller GaP crystallites and growth into larger ones. However, GaP nanocrystallites become unstable under increasing reaction temperatures or prolonged reaction times. EDAX and XRD were used to identify the new Ga_3P phase.

Introduction

Semiconductor nanocrystals have attracted considerable interest since they exhibit a wide variety of intriguing size-dependent properties, such as the blue shift of the optical absorption and photoluminescence, electronic and nonlinear optical effects and fast relaxation times. These properties result from a quantum confinement effect in systems with small dimensions; these dimensions are sensitive to the fabrication method.[1−2] Research on the applications of semiconductor nanometer materials, such as biological fluorescence marking[3] and optoelectronic devices, has also been greatly promoted.[4−5] In addition, the high surface area and the specific growth kinetics can also influence the interior structure of nanocrystals. In order to use these effects, however, it is important to control the size and the size distribution, as well as the stability of the particles against conglomeration. The structural, physical, electronic and magnetic properties may be controlled by changing the synthetic method.

Increasing progress has been made on the research and development of semiconductor nanometer materials.[6] Among the semiconductor materials, the group II−VI compounds have been studied the most widely. Much work has been done on them, especially on aspects of their preparation and properties.[7−10] The core/shell nanostructures of the II−VI materials have also been studied because the shell type and shell thickness provide further control for tailoring the optical, electronic, electrical, and chemical properties of semiconductor nanocrystals.[11−14] In contrast, III−V semiconductor nanoscale materials are less well studied because the II−VI semiconductors are easier to prepare, for a number of reasons.[15] Current interest has focused on the synthesis and characterization of III−V semiconductor nanocrystals and the optical properties of quantum size particles.[16−18] III−V semiconductor nanowires have attracted much interest in recent years for their potential application in high-electron-mobility nanoelectronic devices and full-color flat panel displays.[19] Several approaches have been successfully developed for the fabrication of these nanowires.[20−24] The morphology, microstructure and the growth mechanism of the nanowires has been investigated in detail.

The most important route for the formation of the III−V semiconductor nanocrystals involves organometallic reagents.[25−29] The solvothermal synthetic route has been studied extensively and has proven to be a powerful route for the preparation of new materials,[30−32] in particular for the preparation of III−V semiconductor nanocrystals.[33−36] The advantage of this method is the effective prevention of the oxidation of the products, with the result that the isolated crystalline materials do not need subsequent treatment at high temperatures. In addition, organometallic precursors are not required. However, since the reaction takes place in a sealed system, relatively little work has been done with regards to the growth process and the stability of the product in the solvothermal process, which in fact influences their application directly.[37]

GaP is an indirect-gap semiconductor and has many important uses in microelectronic devices. A few reports have been published on the synthesis and properties of GaP nanocrystals[25,38−39] and nanowires.[28,29] In previous work, we have reported on the factors that affect the particle size of GaP nanocrystals in the reactions of both $GaCl_3{\cdot}Et_2O$ and $GaCl_3$·benzene with Na_3P, where the GaP nanorods and nanospheres were synthesized under solvothermal conditions in benzene.[40,41] It is necessary to study the growth

[a] Structure Research Laboratory and Department of Chemistry, University of Science and Technology of China, Hefei, Anhui 230026, P. R. China
Fax: (internat.) + 86-551/360-3987
E-mail: yxielab@ustc.edu.cn

  DOI: 10.1002/ejic.200200647

mechanism and the stability of nanoparticles under different synthetic conditions in order to determine the best method of synthesis. As far as we are aware, the synthesis of Ga_3P nanocrystals has not been reported previously, although the electronic state of Ga_3P clusters has been studied theoretically.[42] It is clear that in the smaller clusters the P−P bond plays a more decisive role in the structure and bonding, however, as the cluster size increases beyond four atoms, the magic stability of P_4 can be overcome by the Ga−P bonds and thus a mixed cluster is expected to exhibit greater stability. We have previously studied the stability of GaP nanocrystals under solvothermal conditions in benzene,[43] but the growth process and the formation mechanism were not discussed.

In this paper, the growth process and stability of GaP nanocrystals under solvothermal conditions in benzene are investigated in detail. A method for controlling the reaction process and improving the uniformity of the GaP grains is presented, as well as the formation of the Ga_3P nanocrystals.

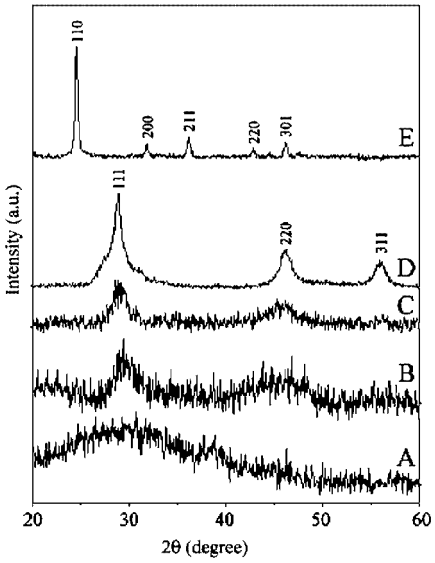

Figure 1. XRD patterns of samples obtained at 300 °C for different reaction times of the mixture: 0 h (A), 3 h (B), 7 h (C), 12 h (D), 24 h (E)

Results and Discussion

The Formation and Growth of GaP Nanocrystals

The reaction was carried out at 300 °C and a series of changes was experienced over different time periods. Figure 1 (A) shows the XRD pattern of the product obtained from mixing the starting materials Na_3P and $GaCl_3$ in a benzene solution, at room temperature. A bump centered at 29° can clearly be seen, which corresponds to the (111) diffraction peak of the GaP crystal with a zincblende structure, indicating the existence of many GaP particles that are small in size. As the reaction proceeds, the bump center becomes weaker from B to D, whereas the three diffraction peaks corresponding to (111), (220) and (311) of the zincblende GaP grow stronger and narrower. However, when the reaction time is increased to 24 h, a new phase appears, indicating that GaP nanoparticles have undergone a chemical change [Figure 1 (E)]. The average size of the GaP crystallites of samples A, B, C and D were calculated to be about 2, 8, 11 and 48 nm, respectively, by the Scherrer equation, which indicates that the particle size enlarges with increasing reaction time.

In order to study the grain size distribution and its change during the reaction, the absorption spectra of samples A, B, C and D were analyzed, which are shown in Figure 2. The absorption peak positions and shape reflect the particle sizes and granularity distribution. The spectrum of sample A is only an inconspicuous peak at about 400 nm, indicating the amorphous nature of A. The absorption spectra of samples B and C show several broad peaks, indicating that there is a broad granularity distribution of GaP nanocrystallites. The absorption edge shifts progressively to the red due to the growth of grains during the reaction process. Although the XRD data indicate larger average particle sizes, this could not be verified by UV/Vis studies. Because there is a broad granularity distribution of GaP nanocrystallites, large numbers of the GaP nanocrystallite particles are smaller than the Bohr radius of the exciton in GaP. So, in the absorption spectra of samples B and C, the broad excitonic peaks arise due to the quantum confinement effect Definitive evidence of the nanoscale dimensions of the quantum particles was obtained from our TEM studies.

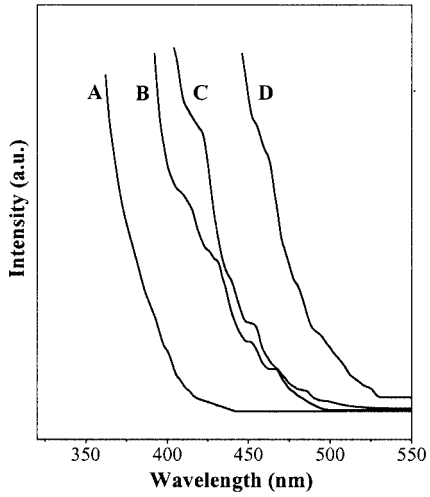

Figure 2. Optical absorption spectra of samples A, B, C and D of Figure 1; sample dispersion in benzene

The morphology of the as-prepared nanoparticles was studied by Transmission Electron Microscopy (TEM), as shown in Figure 3. Figure 3 (A) shows the morphology of the product of sample A. In sample B there are very few large crystallites but a large amount of smaller ones. Compared with sample B, the proportion of large crystallites increases in sample C and the granularity distribution is irregular, although many smaller particles also exist. The

shape of these nanoparticles is nearly spherical with diameters ranging from 5 to 10 nm for sample B and 8 to 16 nm for sample C, in accordance with the average size estimated from the XRD patterns. Because there are so many smaller particles, the excitonic peaks arise in our UV/Vis studies for samples B and C. The proportion of smaller crystallites in sample D is reduced and the grains become uniform. As in sample C, the GaP particles are essentially spherical and the average diameter is nearly 46 nm, which is also consistent with the calculated crystallite sizes from XRD patterns. Figure 3 (E and F) represent the selected area electron diffraction (SAED) of samples A and D, respectively. Figure 3 (E) shows one electron diffraction ring and (F) shows three electron diffraction rings corresponding to the zincblende phase. The SAED results are consistent with the XRD results. Figure 3 (E) indicates that the diffraction bump centered at 29° in Figure 1 (A) corresponds to the (111) diffraction peak of a GaP crystal with a zincblende structure.

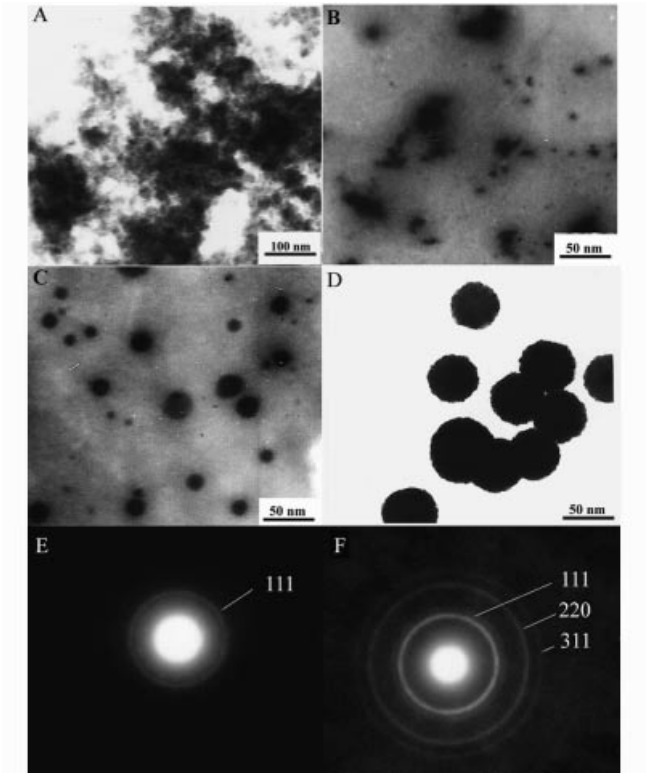

Figure 3. TEM images for GaP nanocrystals prepared at 300 °C for different reaction times of the mixture: 0 h (A), 3 h (B), 7 h (C), 12 h (D); E and F are the SAED patterns of samples A and D

From the XRD, UV/Vis absorption spectra and TEM images, it is clear that samples B and C consist mainly of smaller crystallites with few large ones present. A mass transport process should exist between these crystallites under high-temperature-high-pressure (HTHP) solvothermal conditions in benzene. This phenomenon can be explained as follows, according to the Kelvin equation [Equation (1)], (where P_0 and P_r are the equilibrium vapor pressure of constituents on the surface of the bulk crystal and nanocrystals with radius r, respectively, σ is the surface tension, ρ is the density of nanocrystals, R is a constant, T is absolute temperature and M is the molecular mass) it is obvious that P_r increases rapidly with a decrease of r.

$$P_r = P_0 \exp\left(\frac{2\sigma M}{\rho R T r}\right) \quad (1)$$

P_r on the surface of the smaller GaP crystallites is larger than it is for the larger crystallites. The different values of P_r for crystallites with different radii is the driving force for the transport of Ga and P from the surface of smaller crystallites to the larger ones. For GaP nanocrystallites, the smaller grains dissolve because of the unsaturation condition near the surface, while the larger grains increase in size due to the supersaturation condition.

From the discussion mentioned above, we propose a method for controlling the transport of the constituents and improving the uniformity of the grain size. As we know, at high monomer concentration the smaller particles grow faster than the larger ones and, as a result, the size distribution becomes more uniform. Therefore, we can raise the concentration of Ga and P in the reaction system to create supersaturation of Ga and P at the surface of the small crystallites as well as the large ones. Assuming that the additional concentration of Ga and P are $[Ga]_{av}$ and $[P]_{av}$, the equilibrium concentrations of the corresponding constituents on the surface of the large crystallites are $[Ga]_{le}$ and $[P]_{le}$, and the values on the surface of the small crystallites are $[Ga]_{se}$ and $[P]_{se}$. The real concentrations of Ga and P are as follows:

Small crystallites: $[Ga]_s = [Ga]_{se} + [Ga]_{av}$, $[P]_s = [P]_{se} + [P]_{av}$

Large crystallites: $[Ga]_l = [Ga]_{le} + [Ga]_{av}$, $[P]_l = [P]_{le} + [P]_{av}$

It is obvious that $[Ga]_l < [Ga]_s$ and $[P]_l < [P]_s$. For the reaction Ga + P $\rightleftarrows$ GaP, the speed (v) is described in Equation (2), where v is the growth speed of crystallites and k is a constant.

$$v = k\,[Ga] \times [P] \quad (2)$$

Thus, the growth speed of the smaller crystallites is faster than that of the larger ones. As a result, the uniformity of the grains improves. This ability to control the uniformity of the semiconductor nanocrystalline grains affords an opportunity to further test theories of quantum confinement and yields samples with desirable optical characteristics suitable for practical application. More experiments were performed to provide further evidence in order to draw better conclusions. Samples A and B are obtained when the concentrations of the precursors are twice those of the first experiments, at 300 °C for 4 h and 6 h, respectively. TEM images of the above samples are shown in Figure 4 (A and B). Figure 4 (C and D) are the images, under the same experimental conditions, where the concentrations of the pre-

cursors are the same as those of the first experiments. It can be seen from the images of samples A and B that the grain size is more uniform than in the samples formed at 300 °C for 4 h and 6 h at lower concentrations. From the TEM images of samples C and D one can see the aggregation of the particles, confirming our previous assumptions. This phenomenon is in accordance with the results obtained from the absorption spectra. The absorption spectra of samples A and B were analyzed and the results are shown in Figure 5. The absorption spectra are regular, with a single absorption peak indicating the uniformity of the particle sizes. The particle sizes of samples A and B are about 5 and 9.5 nm, respectively. The Bohr radius of the exciton is reported to be 55 Å (a diameter of 11 nm) in GaP.[44] The absorbance peaks at 380 nm [Figure 5 (A)] and 416 nm [Figure 5 (B)] correspond to approximately 5 and 9 nm GaP crystallites, respectively, which is consistent with the TEM results.

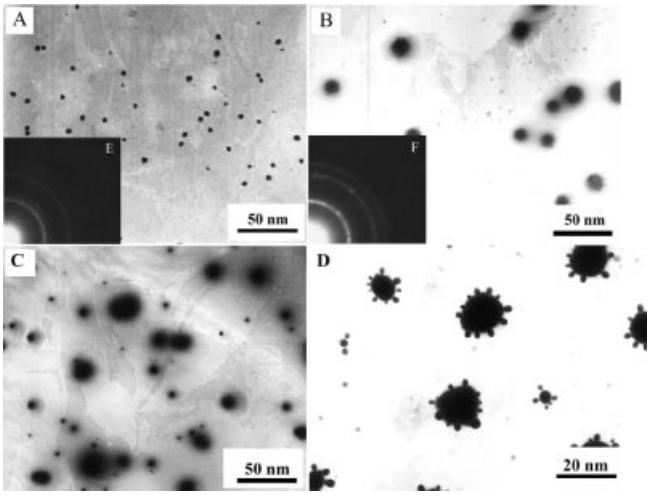

Figure 4. TEM images for GaP nanocrystals prepared at 300 °C at twice the precursor concentrations for 4 h (A), 6 h (B); C and D are the TEM images for GaP nanocrystals prepared at four times the precursor concentrations for 4 h and 6 h; the insets E and F are the SAED pattern of samples A and B

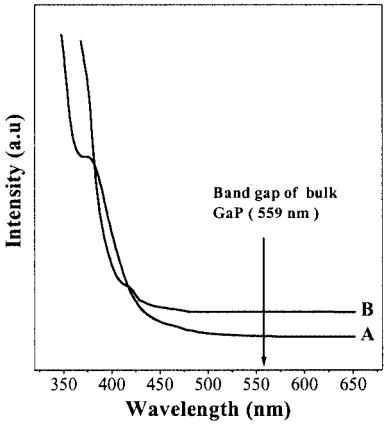

Figure 5. Optical absorption spectra of samples A and B of Figure 4

The Stability of GaP Nanoparticles and the Formation of Ga_3P Nanocrystals

In the previous section it could be seen that a new phase was obtained after Na_3P and $GaCl_3$ reacted at 300 °C for 24 h. The XRD pattern of this new phase is shown in Figure 1 (E). An Energy Dispersive X-ray Diffraction (EDAX) analysis study was performed in order to determine the composition of sample E, obtained at 300 °C over 24 h. Figure 6 shows the EDAX spectrum, in which both P and Ga bands are detected when the electron beam is focused on one of the particles. Na and Cl were also detected because the sample was not properly washed and so an extremely small amount of by-product (NaCl) is present. Because of the low concentration of NaCl and the small particle size, direct determination of the NaCl by X-ray diffraction is difficult; no NaCl diffraction peaks appear in Figure 1 (E). The insert in Figure 6 indicates the results of the elemental analysis. From the EDAX and element analysis, we conclude that the new compound is Ga_3P. Moreover, all the reflections shown in Figure 1 (E) can be indexed to the tetragonal Ga_3P phase and the average crystallite sizes of Ga_3P were found to be about 55 nm, as estimated from the Scherrer formula.

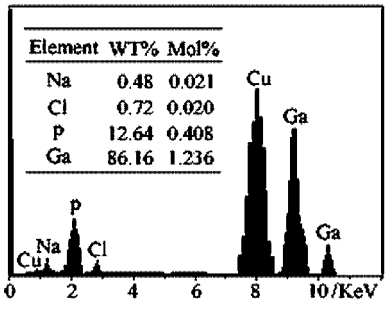

Figure 6. The EDAX results of Ga_3P at 300 °C for 24 h; inset: elemental analysis result of sample E

From the above discussion it can be seen that Ga_3P is obtained from the reaction of Na_3P and $GaCl_3$ at 300 °C for 24 h, indicating that GaP is in fact metastable in the solvothermal process. In order to confirm this metastability, a further series of experiments was performed. All products were identified from the XRD patterns. Figure 7 shows the XRD patterns of the samples that were prepared at 420 °C for 12 h (A), 400 °C for 14 h (B) and 340 °C for 20 h (C). The relationship between the reaction conditions and products is summarized in Table 1. Figure 8 shows the TEM images of Ga_3P, from which one can see that at 420 °C for 12 h (A) or at 400 °C for 14 h (B), Ga_3P nanocrystallites have a high crystallinity and are well distributed. This is better than the results for Ga_3P obtained at 340 °C for 20 h (C) or at 300 °C for 24 h (D). The size distribution of the sample obtained at 300 °C for 20 h is irregular: the largest particle size is 75 nm but the smallest is only 20 nm. This result is consistent with the average particle sizes from the

XRD patterns. Figure 8 (E and F) are the ED patterns of samples A and D. The diffraction intensity gives more proof of the crystallinity of the samples at different temperatures and times.

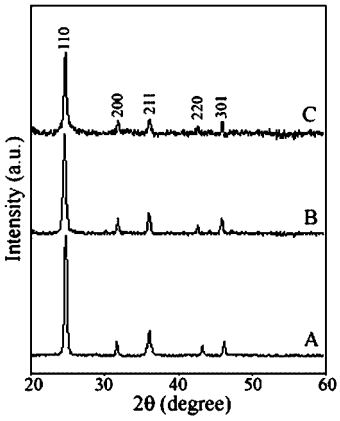

Figure 7. XRD patterns of Ga_3P at 420 °C/12 h (A), 400 °C/14 h (B), 340 °C/20 h (C)

Table 1. Relation between reaction conditions and products

Temp. [°C]	Time [h]	Product
300	7	GaP
	12	GaP
	20	GaP (major), Ga_3P (minor)
	24	Ga_3P
340	8	GaP
	12	GaP (major), Ga_3P (minor)
	20	Ga_3P
380	8	GaP
	12	GaP (major), Ga_3P (minor)
400	8	Ga_3P (major), GaP (minor)
	14	Ga_3P
420	8	Ga_3P (major), GaP (minor)
	12	Ga_3P

In the current system, GaP was formed by the reaction $Na_3P + GaCl_3 \rightarrow GaP + 3\ NaCl$, but upon prolonging the reaction time or increasing the reaction temperature, the products turned into Ga_3P. Careful observation showed that, after heating at 300 °C for between 3 and 12 h, the autoclave was filled with a blue-green benzene solution and a gray-black powder (GaP), whereas when the heating time reached 24 h at 300 °C, 20 h at 340 °C, 14 h at 400 °C or 12 h at 420 °C, the autoclave was filled with a yellow or light-brown benzene solution and a gray-white powder (Ga_3P). Upon removing some of the yellow or light-brown benzene solution and dripping it onto filter paper in air, spontaneous combustion takes place, indicating that white phosphorus is dissolved in the yellow or light-brown benzene solutions. In our experiments the Na_3P and $GaCl_3$ molar ratio is 1:1, so we believe that under solvothermal conditions in benzene, the decomposition of GaP should take place when the reaction time is prolonged or the reaction temperature is increased as shown in Equation (3).

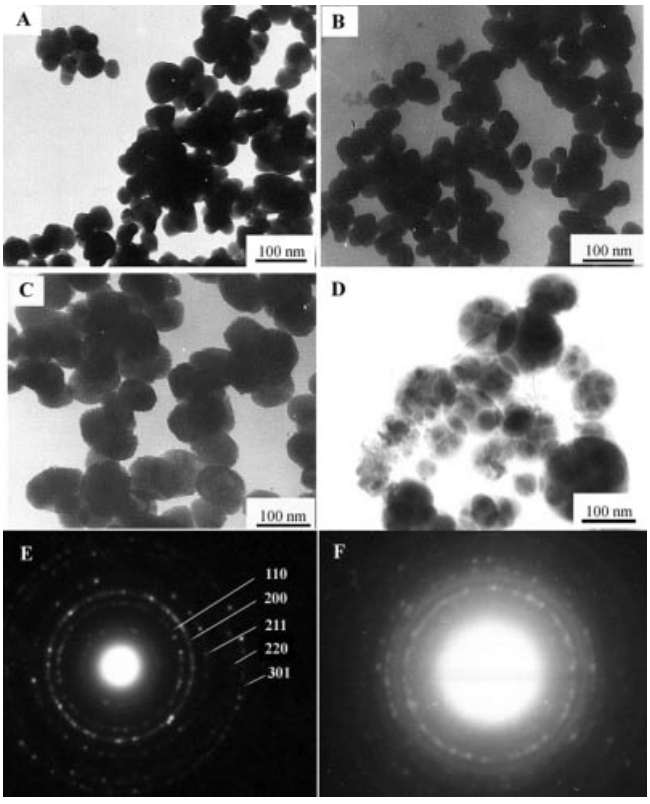

Figure 8. TEM images of Ga_3P at 420 °C/12 h (A), 400 °C/14 h (B), 340 °C/20 h (C), 300 °C/24 h (D); E and F are the SAED pattern of samples A and D

$$6\ GaP \rightarrow 2\ Ga_3P + P_4 \quad (3)$$

In order to study the reaction mechanism, more experiments were performed. A purified sample of GaP was placed into an autoclave, under the same solvothermal conditions; the results differed from the above-mentioned results. Thus, either NaCl or unchanged Na_3P is necessary for the decomposition process to occur.[45−47]

Experimental Section

Preparation and Growth of GaP Nanocrystals: All analytical grade solvents used in our experiments were dried with sodium chips and distilled under a flow of N_2. All reagents were analytical grade or better and used without any purification, except for Na_3P, which was prepared according to the literature (small pieces of sodium and an excess of white phosphorus were mixed in benzene, heated to the melting point of sodium, and stirred and refluxed for 10−12 h).[48] A typical experimental procedure is as follows: Na_3P powder and a benzene solution of $GaCl_3$ were placed in a stainless steel autoclave and benzene was added to raise its ratio to 70−85%. After the air in the solution was expelled by N_2 (99.999% pure), the autoclave was sealed and heated to 300 °C over different time

periods, and then allowed to cool to room temperature. The products were filtered off and washed with benzene, absolute ethanol and distilled water. Finally, the products were dried under vacuum at room temperature for 2 h. In order to study the growth and stability of GaP nanoparticles the as-prepared GaP was treated at different temperatures and times under the same conditions.

Characterization of the Products: The phases of the products were detected at a scanning rate of $0.02°s^{-1}$ in the 2θ range from 20 to 60° by using a *D*/max-γA X-ray diffractometer with Ni-filtered Cu-K_α radiation. Optical absorption spectra were recorded with a Hitachi 340 UV/Vis/NIR recording spectrophotometer at room temperature. The absorption cell used was a 1-cm quartz cuvette. A blank solution of benzene was used as the reference. TEM images of the samples were obtained from a Hitachi model H800 transmission electron microscope using an accelerating voltage of 200 kV. To prepare the TEM samples, the colloids were briefly ultrasonicated, and then a drop of the colloidal suspension was applied to a copper mesh covered with a carbon film for 30 s.

Acknowledgments

Financial support from the National Natural Research Foundation of China and Chinese Ministry of Education is gratefully acknowledged. We are indebted to Prof. G. E. Zhou and Dr. X. M. Liu for their help with the XRD and TEM analyses.

[1] C. B. Murray, C. R. Kagan, M. G. Bawnedi, *Annu. Rev. Mater. Sci.* **2000**, *30*, 545 and references therein.
[2] U. Banin, Y. W. Cao, D. Katz, O. Millo, *Nature* **1999**, *400*, 542.
[3] G. P. Mitchell, C. A. Mirkin, R. L. Letsinger, *J. Am. Chem. Soc.* **1999**, *121*, 8122.
[4] M. C. Schlamp, X. G. Peng, A. P. Alivisatos, *J. Appl. Phys.* **1997**, *82*, 5837.
[5] D. L. Klein, R. Richard, A. K. L. Lin, A. P. Alivisatos, P. L. McEuen, *Nature* **1997**, *389*, 699.
[6] T. Trindade, P. O'Brien, N. L. Pickett, *Chem. Mater.* **2001**, *13*, 3843 and references therein.
[7] X. Peng, M. C. Schlamp, A. V. Kadavanich, A. P. Alivisatos, *J. Am. Chem. Soc.* **1997**, *119*, 7019.
[8] A. P. Alivisatos, P. F. Barbara, A. W. Castleman, J. Chang, D. A. Dixon, M. L. Klein, G. L. McLendon, J. S. Miller, M. A. Ratner, P. J. Rossky, S. I. Stupp, M. E. Thompson, *Adv. Mater.* **1998**, *10*, 1297.
[9] A. L. Rogach, S. V. Kershaw, M. G. Burt, M. T. Harrison, A. Kornowski, A. Eychmüller, H. Weller, *Adv. Mater.* **1999**, *11*, 552.
[10] M. A. Anderson, S. Gorer, R. M. Penner, *J. Phys. Chem. B* **1997**, *101*, 5895.
[11] M. T. Harrison, S. V. Kershaw, A. L. Rogach, A. Kornowski, A. Eychmuller, H. Weller, *Adv. Mater.* **2000**, *12*, 123.
[12] Y. W. Cao, U. Banin, *Angew. Chem. Int. Ed.* **1999**, *38*, 3692.
[13] B. Schreder, T. Schmidt, V. Ptatschek, U. Winkler, A. Materny, E. Umbach, M. Lerch, G. Müller, W. Kiefer, L. Spanhel, *J. Phys. Chem. B* **2000**, *104*, 1677.
[14] D. Hagrman, C. Zubieta, D. J. Rose, J. Zubieta, R. C. Haushalter, *Angew. Chem. Int. Ed. Engl.* **1997**, *36*, 873.
[15] J. R. Heathand, J. J. Shiang, *Chem. Soc. Rev.* **1998**, *27*, 65.
[16] A. Manz, A. Birkner, M. Kolbe, R. A. Fischer, *Adv. Mater.* **2000**, *12*, 569.
[17] O. I. Micic, S. P. Ahrenkiel, D. Bertram, A. J. Nozik, *Appl. Phys. Lett.* **1999**, *75*, 478.
[18] O. I. Micic, H. M. Cheong, H. Fu, A. Zunger, J. R. Spragus, A. Mascarenhas, A. J. Nozik, *J. Phys. Chem. B* **1997**, *101*, 4904.
[19] X. F. Duan, Y. Huang, Y. Cui, J. F. Wang, C. M. Lieber, *Nature* **2001**, *409*, 66.
[20] W. S. Shi, Y. F. Zheng, N. Wang, C.-S. Lee, S.-T. Lee, *Adv. Mater.* **2001**, *13*, 591.
[21] C.-C. Chen, C.-C. Yeh, *Adv. Mater.* **2000**, *12*, 738.
[22] X. Duan, J. Wang, C. M. Lieber, *Appl. Phys. Lett.* **2000**, *76*, 1116.
[23] X. Duan, C. M. Lieber, *Adv. Mater.* **2000**, *12*, 298.
[24] M. S. Gudiksen, C. M. Lieber, *J. Am. Chem. Soc.* **2000**, *122*, 8801.
[25] R. J. Jouet, R. L. Wells, A. L. Rheingold, C. D. Incarvito, *J. Organomet. Chem.* **2000**, *601*, 191.
[26] X. Peng, J. Wickham, A. P. Alivisatos, *J. Am. Chem. Soc.* **1998**, *120*, 5343.
[27] M. Green, P. O'Brien, *Chem. Commun.* **1998**, 2459.
[28] R. Cohen, L. Kronik, A. Shanzer, D. Cahen, A. Liu, Y. Rosenwaks, J. K. Lorenz, A. B. Ellis, *J. Am. Chem. Soc.* **1999**, *121*, 10545.
[29] A. Manz, A. Birkner, M. Kolbe, R. A. Fischer, *Adv. Mater.* **2000**, *12*, 8.
[30] W. S. Sheldrick, M. Wachhold, *Angew. Chem. Int. Ed. Engl.* **1997**, *36*, 206.
[31] J. Yang, J. H. Zeng, S. H. Yu, L. Yang, G. E. Zhou, Y. T. Qian, *Chem. Mater.* **2000**, *12*, 3259.
[32] A. Holllingsworth, D. M. Poojary, A. Clearfield, W. E. Buhro, *J. Am. Chem. Soc.* **2000**, *122*, 3562.
[33] L. Grocholl, J. J. Wang, E. G. Gillan, *Chem. Mater.* **2001**, *13*, 4290.
[34] S. D. Dingman, N. P. Rath, P. D. Markowitz, P. C. Gibbons, W. E. Buhro, *Angew. Chem. Int. Ed.* **2000**, *39*, 1470.
[35] Y. Xie, Y. Qian, W. Wen, S. Zhang, Y. Zhang, *Science* **1996**, *272*, 1926.
[36] J. Jegier, S. McKernan, A. P. Purdy, W. L. Gladfelter, *Chem. Mater.* **2000**, *12*, 1003.
[37] C. C. Chen, A. B. Herhold, C. S. Johnson, A. P. Alivisatos, *Science* **1997**, *276*, 398.
[38] S. S. Kher, R. L. Wells, *Chem. Mater.* **1994**, *6*, 2056.
[39] O. I. Micic, J. R. Sprague, C. J. Curtis, K. M. Jones, J. L. Machol, A. J. Nozik, H. Giessen, B. Fluegel, G. Mohs, N. Peyghambarian, *J. Phys. Chem.* **1995**, *99*, 7754.
[40] S. M. Gao, D. L. Cui, B. B. Huang, M. H. Jiang, *J. Cryst. Growth* **1998**, *192*, 89.
[41] S. M. Gao, Y. Xie, J. Lu, G. A. Du, W. He, D. L. Cui, B. B. Huang, M. H. Jiang, *Inorg. Chem.* **2002**, *41*, 1850.
[42] P. Y. Feng, K. Balasubramanian, *Chem. Phys. Lett.* **1998**, *288*, 1.
[43] C. Y. Xin, S. M. Gao, D. L. Cui, B. B. Huang, X. Y. Qin, M. H. Jiang, *Acta Phys.-Chim. Sin.* **1999**, *15*, 105.
[44] M. V. Ramakrishna, R. A. Friesner, *J. Chem. Phys.* **1991**, *95*, 8309.
[45] D. S. Tin, T. Miller, T. C. Chiang, *Phys. Rev. B* **1991**, *44*, 10719.
[46] H. Ishida, K. Terakura, *Phys. Rev. B* **1989**, *40*, 11519.
[47] R. Ramfrez, *Phys. Rev. B* **1989**, *40*, 10144.
[48] D. J. Peterson, Y. J. Logan, *J. Inorg. Nucl. Chem.* **1966**, *28*, 53..

Received November 25, 2002

